

**Synthesis of Morphine Loaded Hydroxyapatite Nanoparticles (HAPs) and  
Determination of Genotoxic Effect for Using Pain Management**

**Abstract**

Morphine is used as a standard analgesic for intensive pain relief. It relieves acute and chronic pain by acting directly on the central nervous system and to treat myocardial infarction and shortness of breath. However, the use of morphine for the alleviation of chronic pain is controversial because of its adverse side effects. The overall success of this medicine in chronic therapy is due to the long-term activity of the drug at a reasonable concentration. Nanoparticle-based carriers have emerged as a new class of drug delivery systems that can overcome traditional drug side-effect limitations by reducing toxicity to a minimum. In this study, a morphine-loaded HAPs drug delivery system was investigated. Fourier Transform Infrared Spectroscopy (FTIR) analysis was used to characterize typical functional groups found in the chemical composition of Hydroxyapatite Nanoparticles (HAPs) and morphine loaded HAPs (HAP+M). Scanning electron microscopy (SEM) and Transmission electron microscope (TEM) analyses were performed to examine the size, morphology, and porosity of morphine loaded HAPs. Characterization analysis showed that HAP nanoparticles were loaded with morphine. The effects of pH on release of morphine-loaded HAPs was determined. The release time of the entrapped morphine in the nanoparticle increased in all conditions, thus increasing the morphine time in the human body. Thus, patients will have to take less morphine. In addition, it was investigated whether the morphine loaded HAP cell produced oxidative stress and genotoxic effect on DNA. Findings presented in this paper suggested that morphine-loaded HAPs have a promising future as a nanocarrier for pain treatment.

**ABBREVIATIONS**

**COMET** : Single-Cell Gel Electrophoresis

**FTIR** : Fourier Transform Infrared Spectroscopy

**HA** : Hydroxyapatite

**HAP+M** : Morphine Loaded Hydroxyapatite Nanoparticles

**HAPs** : Hydroxyapatite Nanoparticles

**HPLC** : High Performance Liquid Chromatography

33 IASP : International Association for the Study of Pain

34 SEM : Scanning electron microscopy

35 TEM : Transmission electron microscope

36 USP : United States Pharmacopeia

37 WHO : World Health Organization

38 TAS : Total Antioxidant Status

39 TOS : Total Oxidant Status

40 OSI : Oxidative Stress Index

41

42

43 **Keywords:** Delivery system, HAPs, Morphine, Pain therapy.

44

45

## 46 1. INTRODUCTION

47

48

49 Accomplish pain management provides adequate analgesia without extreme side effects. The  
50 current pain management method of the World Health Organization (WHO) begins with non-  
51 opioid drugs, progresses with weak opioids and results in strong opioids [1]. The WHO also  
52 suggests adjuvant treatment with antidepressant drugs to help decrease anxiety associated  
53 with chronic pain. Pain management can be complicated by the dependence on the drugs used  
54 and drug side effects. Many factors can influence the drug trend, including genetic diversity,  
55 which can further complicate the management of these factors [2]. Morphine is a powerful  
56 pain reliever and is used to treat severe pain such as surgery, serious injury, cancer-related  
57 pain, or heart attack. It is also used for other chronic pain types where weaker painkillers are  
58 no longer effective. Morphine is marketed in the form of tablets, capsules, granules,  
59 injectable, and suppositories and can only be used by prescription. It is used as a standard  
60 analgesic for intensive pain treatment. It is used directly to relieve acute and chronic pain by  
61 acting on the central nervous system. It works by preventing the pain signals moving along  
62 the nerve from passing to the brain [3].

63

64 However, the use of morphine for the alleviation of chronic pain is controversial because of  
65 the adverse side effects such as addiction, respiratory depression, gastrointestinal effects, and  
66 urological effects. The most common side effects of morphine are constipation, feeling sick

67 and insomnia. The use of morphine for the treatment of chronic pain can only be confirmed in  
68 patients who do not respond to other treatments. Because the long-term effects of overdose  
69 and continuous use of morphine can affect almost all organ systems of the body [3].

70

71 Over the past several decades, nanotechnology has emerged with momentum as a promising  
72 new solution to a range of previously unsolvable scientific and technological issues.  
73 Nanoparticles offer a massive range of properties and characteristics that can be finely tuned  
74 for many applications, from electronics to medicine. More recently, an exploration into their  
75 uses in the field of targeted drug delivery has gained popularity with many successes and  
76 advancements resulting [4-6]. Even with these successes, there has been a delay in the transfer  
77 of nanotechnology to the field of pain management. Nanoparticles are available in sizes that  
78 are well within the range of typical synaptic gaps through which neurons communicate, and  
79 their size also lends them towards possible passage through the blood-brain barrier, a system  
80 of tight gap junctions which prevent the passage of large, ionized molecules from entering the  
81 central nervous system [7,8]. These size advantages, coupled with the ease of surface  
82 modifications and highly tunable characteristics, suggest that the future of pain management  
83 lies within the field of nanotechnology.

84

85 Hydroxyapatite (HA) is a bioactive, osteoconductive chemical agent that is neither toxic nor  
86 immunogenic [9]. There are several applications of HA such as catalysis, fertilizers and  
87 pharmaceutical products, water treatment processes and bone and tooth repair. However, the  
88 applications areas are very restricted because of their fragility. Many studies have been  
89 carried out to modify HA with polymers since natural bone is a composite consisting  
90 essentially of nano-sized pinhole HA crystals (constituting about 65% of bones) [3] and  
91 collagen fibers [4]. Extremely thin HA powder has been used to increase the quality of HA  
92 [5]. In the literature, a number of methods such as Sol-gel [6,7], reverse microemulsion [8,9],  
93 hydrothermal [10], microwave hydrothermal [11], precipitation [12] and solid-state reaction  
94 [12] have been reported for HA synthesis. Nano-sized and weak agglomerated HA particles  
95 were produced by hydrothermal and microemulsion methods [5]. The most reported method  
96 for preparing HA particles is the precipitation method. This process is easy, economic and  
97 appropriate for industrial production [5]. Ultrasonication is known to be particularly useful for  
98 disrupting aggregates and reducing size and polydispersity of nanoparticles [13].

99

100 HA acts as a prototype for bones and teeth and is also commonly used in medical implants  
101 [14]. HA is used in the bone as nano-sized needle-like crystals. HA can be used in a variety of  
102 forms including powder, granules, porous grains. It is necessary to characterize the HA  
103 powder depending on the desired application. Some parameters such as purity, crystallinity,  
104 and morphology can be controlled when the wet synthesis technique is used. Applications of  
105 morphologies can differ. For example, although spherical particles are used in thermal spray  
106 coating, needle-shaped or rod-shape are used in bone repair composite material [15].  
107 Recently, nano-HA has attracted the attention of researchers thanks to the important role of  
108 HA in several biomedical applications. The nanoparticle size of the HA crystal is an average  
109 length of 50 nm and is embedded in the collagen matrix in natural bone and teeth. Actually,  
110 collagen acts as a template in the collagen-controlled bio-mineralization process [16].

111  
112 A long-acting product formulation from the morphine will have the potency of both patient  
113 rehabilitation and patient comfort. The overall success of this drug in chronic therapy is due to  
114 its long-term activity at a reasonable concentration around the action area. After entering the  
115 host, the nanoparticles, which have a reasonable density near the domain, function as a drug  
116 reservoir capable of releasing the drug for a long time in the bloodstream. This long-acting  
117 drug profile is used as a basis for long-term chronic drug action to the desired effect. For these  
118 reasons, there is a need to develop a morphine-loaded nanoparticle drug release system  
119 without any cytotoxicity threat. In addition, there is a need to be developed to release the  
120 morphine loaded drug slowly and in a controlled manner into the action zone.

121  
122 In this study, the first time morphine loaded HAPs (HAP + M) were synthesized and partial  
123 characterization was performed. The effect of morphine release of pH was investigated and  
124 the genotoxicity of HAP + M was determined by comparing the comet assay and oxidative  
125 stress parameters.

126

## 127 **2. MATERIALS AND METHODS**

128

### 129 **2.1. Materials**

130 Poppy capsules were obtained from Opium Alkaloid Plant (Turkish Grain Board). The  
131 capsules were broken and their seeds are separated. Poppy capsules were dried at room  
132 temperature for 15 days in a dark room at room temperature. It was ground to the size of 80  
133 mesh grain size before extraction. Morphine Reference Standard was obtained from the

134 United States Pharmacopeia (USP). All chemicals used in all experiments were in analytical  
135 quality and in High performance liquid chromatography (HPLC) grades all solvents used for  
136 chromatographic purposes. All chemicals were purchased from Sigma Aldrich. 0.45 µm  
137 membranes (Millipore, Bedford) were used for the filtration of all solutions.

138

## 139 **2.2. Extraction of morphine from poppy capsules.**

140 Alkaloids are produced by using natural products or synthetically. Because of the low toxicity  
141 of natural products, they are preferred from the pharmaceutical industry. Therefore, morphine  
142 was extracted from poppy capsules in this study. 100 gr. of dried and the ground sample was  
143 weighed into a 2 lt. of the beaker. 1000 ml. of solvent (80 % Methanol + 20 % 0.1 M. HCl)  
144 was added over the capsules. Morphine was extracted for one day by constant stirring. The  
145 mixture was filtered off. 500 ml. of solvent (80 % Methanol + 20 % 0.1 M. HCl) was added  
146 on the poppy capsules for the second extraction. The mixture was filtered off. 500 ml. of  
147 solvent (80 % Methanol + 20 % 0.1 M. HCl) was added on the poppy capsules for the third  
148 extraction. The mixture was filtered off. All extracts obtained from three extractions were  
149 combined for purification. The combined extract was evaporated under vacuum at 40 °C in a  
150 rotary evaporator to 200 ml. of a total volume. 200 ml. of concentrated aqueous extract was  
151 left. Concentrated extract was kept in the refrigerator for one day. The extracts were filtered  
152 and plant-derived wax, tannins, and oily substances were separated and thrown. A small  
153 amount of diatomaceous earth was added to remove the impurities in the concentrated extract  
154 solution to obtain a clearer extract, and the mixture was stirred at 50 °C for half an hour. The  
155 mixture was filtered through white band strainer paper. A more transparent extract was  
156 obtained.

157

158 The concentrated extract was extracted 3 times with petroleum ether to remove the vegetative  
159 oily substances in the concentrated extract. In each extraction, the aqueous concentrate extract  
160 and the petroleum ether were stirred for 15 min. It was left for 15 min. and the phases were  
161 allowed to separate. The morphine-free petroleum ether phase was discarded. Active carbon is  
162 used to remove undesirable compounds that can cause color, quality, and property changes in  
163 liquids due to its enabling feature of final product in the pharmaceutical industry to be  
164 uncolored and purified. For this, a small amount of activated carbon was added to the extract,  
165 stirred at 50 °C for half an hour and filtered. This process was repeated three times. Finally,  
166 the concentrated extract was evaporated to a saturation concentration in a rotary evaporator.  
167 The amount of morphine in the concentrated extract was determined by HPLC analysis [17].

168

### 169 **2.3. Preparation of morphine loaded HAPs with precipitation method using ammonium** 170 **phosphate and calcium nitrate solutions**

171 HAPs were prepared using an aqueous precipitation technique. The molar concentration of  
172 calcium nitrate tetrahydrate and diammonium hydrogen orthophosphate was adjusted to have  
173 a theoretical value of the Ca/P ratio: 1.667. 0.156 M stock solution of diammonium hydrogen  
174 orthophosphate in demineralized water and 0.400 M stock solution of calcium nitrate  
175 tetrahydrate in absolute ethanol were used. These solutions were continuously mixed at a  
176 temperature of 70 °C for 4 hrs. on the magnetic stirrer. 100 ml of diammonium hydrogen  
177 orthophosphate solution was added to the beaker to synthesize morphine-loaded HAPs. The  
178 solution was heated to 70 °C. 50 ml of concentrated morphine solution was added over it.  
179 100 mL of the calcium nitrate solution was added dropwise to this mixture for an hour. The  
180 mixture was stirred at 70 °C for 4 hours. The precipitated white colored nanoparticles were  
181 filtered using white band filter paper and washed three times with double distilled water and  
182 finally with ethanol. Nanoparticles powder were dried in an oven at 105 °C for 4 hours until it  
183 gets dry.

184

### 185 **2.4. Characterization Analysis of HAPs**

#### 186 **2.4.1. Determination of Morphine Contents by HPLC Analysis**

187 In our study, HPLC analyzes were used to determine that morphine content was loaded into  
188 HAP. Therefore, Purity control was not carried out in the extraction steps. Chromatographic  
189 analyzes were performed on an Agilent brand 1260 model HPLC instrument (Agilent, USA).  
190 The system includes a quaternary gradient pump, vacuum degasser, column thermostat,  
191 automatic sampler, and (UV/VIS) detector. The Chem. Station software was used to collect  
192 and evaluate data. Chromatographic separation was performed with an ACE C18 column (5  
193 µm, 150 mm. X 4.6 mm. I. D.). Mobile phase A was a solution of 5 % acetonitrile and mobile  
194 phase B was a mixture of acetonitrile: glacial acetic acid: trimethylamine in the ratio of (97.9:  
195 2: 0.1, v/v). The flow rate of the mobile phase was 1 ml./min.; Column thermostat  
196 temperature was maintained at 30 °C; Injection volume was 50 µl. Detection was carried out  
197 at 284 nm; Working time: 30 min. Elution was performed with the gradient: 0 min. 10%  
198 solvent B; 0–5 min. from 10 to 15% solvent B; 5–10 min. from 15 to 20% solvent B; 10–  
199 20 min. from 20 to 35% solvent B; 20–30 min. from 35 to 10% solvent B [18].

200

201 To analyze the amount of morphine in the morphine-loaded nanoparticle, 200 mg. of  
202 nanoparticle was weighed into a 100 ml. beaker. 20 ml. of 0.1 M. HCl was added and  
203 dissolved in the ultrasonic bath. Transferred to a 50 ml. balloon, the volume was completely  
204 deionized water. The amount of morphine in the resulting solution was analyzed by HPLC.

205

#### 206 **2.4.2. Fourier-transform infrared spectroscopy (FTIR), Scanning electron microscopy** 207 **(SEM) and Transmission electron microscopy (TEM) analysis**

208 FTIR analysis was carried out to determine the various phosphate and carbonate functional  
209 groups in the synthesized HAPs. HAPs dried at 105 °C was analyzed for FTIR analysis.  
210 Spectrum Two model of Perkin Elmer brand FTIR Spectrometer was used in FTIR analysis.

211

212 SEM analysis was performed to determine the morphological and grain sizes of the  
213 synthesized nanoparticles. Phenom brand ProX model SEM device was used in the analysis.

214

215 TEM analysis was performed to clarify the size, shape, morphology and structure of the  
216 nanoparticles. JEOL JEM-2100 transmission electron microscope (UHR) device was used in  
217 the analysis.

218

#### 219 **2.5. The effect of pH on morphine-loaded drug release**

220 A NaCl / HCl solution with a pH of 1.2 (stomach pH) and 7.4 (intestinal pH) were prepared.  
221 The release tests were carried out at a temperature of  $37 \pm 0.5$  °C (human body temperature)  
222 in a horizontal shaking kiln at 100 rpm. 200 mg. powder of morphine loaded HAPs was  
223 weighed to a beaker of 100 ml. and added 20 ml. of the PBS solution. The morphine amount  
224 in the prepared medium is 14.2 ppm. Erlenmeyer was covered with aluminum foil and was  
225 placed in a shaker oven 100 rpm at 37 °C. 2 ml. of samples was taken at every five hours. The  
226 samples were analyzed by HPLC after filtration through an injector filter [19]. Measurements  
227 were continued until the drug release was fixed.

228

#### 229 **2.6. Comet assay**

230 The blood samples were collected from a healthy and non-smoking young donor at the age of  
231 28. Leukocytes were isolated over Histopaque 1083 gradients by centrifugation at 2100 rpm  
232 for 20 min. at 15 °C. The comet assay was performed under alkaline conditions according to  
233 Singh *et al.* (1988) with some modifications. Isolated human leukocytes (100 µL) were  
234 incubated with 100 µL different concentrations of HA and HA+M (5, 10 and 25 mg./ml.) for

235 1 hrs. at 37°C [20]. a Positive (30 mM. H<sub>2</sub>O<sub>2</sub>) and a solvent control (1XPBS) were also  
 236 included. Following the incubation, leucocytes were at 1600 rpm for 10 min. at 25 °C. While  
 237 supernatant was used for TAS and TOS determination, the pellet was used for Comet assay.  
 238 The Comet assay protocol was done according to *Avuloglu-Yilmaz et al. (2017)* [21]. The  
 239 analysis of comet scores was calculated as described by the *Cigerci et al. (2015)* [22].

240

## 241 2.7. Measurement of total oxidant status and oxidative stress index

242 TOS and TAS were determined spectrophotometrically using Rel Assay Diagnostic kit  
 243 RL0024 and RL0017 reading at 530 nm. and 660 nm. respectively by Elisa Thermo Scientific.  
 244 TAS and TOS value was calculated according to the following formula;

245

$$246 \text{TOS: } (\Delta\text{AbsSample}) / (\Delta\text{AbsStandard}) \times \text{Conc. of standard} \quad (1)$$

$$247 \text{TAS: } ((\Delta\text{Abs H}_2\text{O}) - (\Delta\text{Abs Sample})) / ((\Delta\text{AbsH}_2\text{O}) - (\Delta\text{Abs Standart})). \quad (2)$$

$$248 \text{The oxidative stress index (OSI): TOS / TAS.} \quad (3)$$

249

## 250 2.8. Statistical analysis

251 The scores were presented as means ± standard deviation. The levels of significance in  
 252 different treatment groups were analyzed Duncan multiple range tests by using SPSS 23.0  
 253 version for Windows software. P < 0.05 was set as statistical significance.

254

## 255 3. RESULTS AND DISCUSSION

256

### 257 3.1 Morphine Contents of Morphine Loaded Nanoparticles by HPLC

258 As a result of HPLC analysis, the content of morphine in the poppy capsules was determined  
 259 as 281.6 ppm and the content of morphine in the nanoparticle was determined as 14.2 ppm  
 260 (Table 1). The HPLC chromatogram of HAPs was shown in Figure 1. A significant amount of  
 261 morphine peak was observed in the HPLC chromatogram of the solution obtained by  
 262 dissolving HAP nanoparticles in 0.1 M HCl solution. This situation is the clearest evidence  
 263 that morphine molecules are loaded into HAP nanoparticles.

264

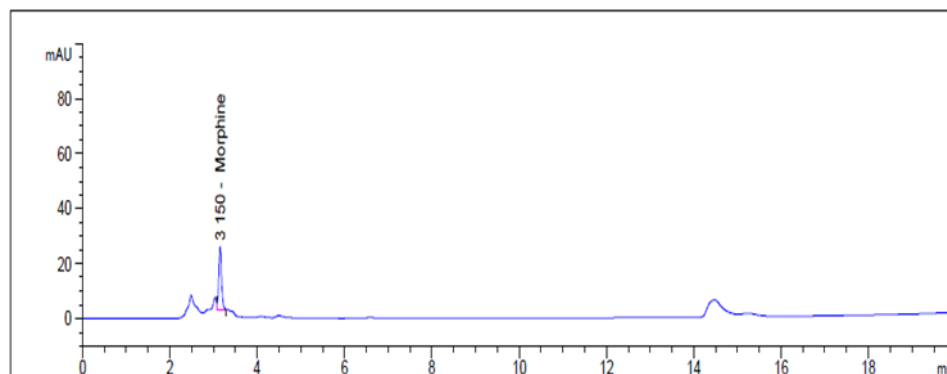
265 **Table 1 The amount of morphine**

Extraction stages	The amount of morphine (ppm)
-------------------	------------------------------



First extraction	281,6
Second extraction	490,5
Third extraction	2872,8
Morphine in the nanoparticle	14,2

266

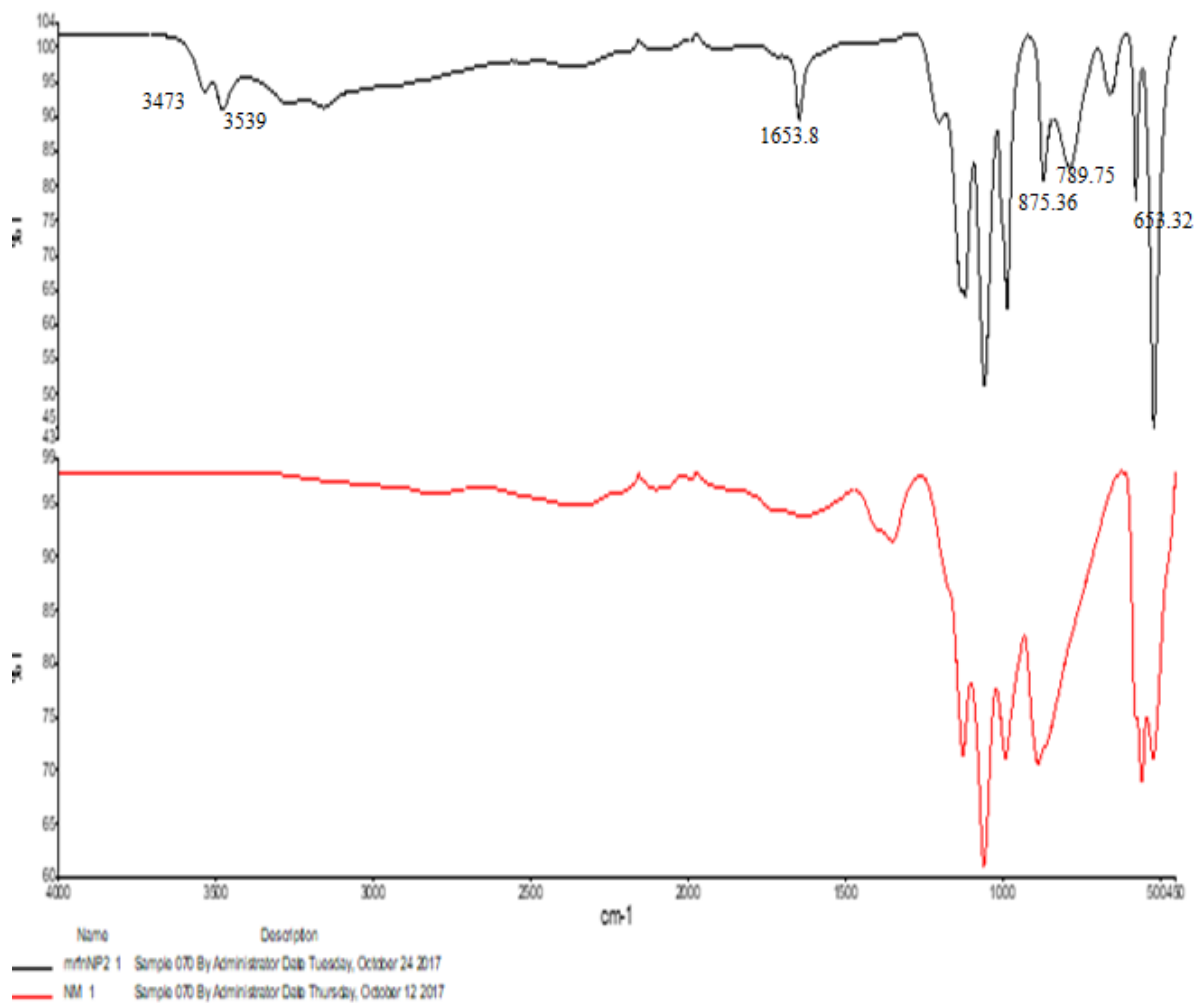


267

268 **Figure 1 HPLC chromatogram of morphine loaded HAPs.**

269

270 Functional groups associated with HA were identified by FTIR spectroscopy. The FTIR  
 271 spectra of morphine loaded HAPs and HAPs were shown in figure 2. The absorption bands at  
 272  $1060\text{ cm}^{-1}$  detected in the spectra are attributed  $(\text{PO}_4)^{3-}$  groups. HA has been revealed by the  
 273 absence of a large peak at  $3550\text{ cm}^{-1}$  attributed to the crystallization water and the water  
 274 molecules trapped in the apatite unit cell. Although non-stoichiometric HA can contain some  
 275 water molecules, stoichiometric HA cannot contain water molecules generally in its unit cell.  
 276 Absorption bands at  $3571\text{ cm}^{-1}$  and  $629\text{ cm}^{-1}$  show the presence of hydroxyl ion in the apatite  
 277 lattice. Absorption bands observed at  $1124, 1060, 993, 886$  and  $562\text{ cm}^{-1}$  show  $(\text{PO}_4)^{3-}$  groups  
 278 [23,24]. *Misra et al (2011)* determined morphine absorption bands in FTIR [25]. Similarly, in  
 279 this study; FTIR spectrum of morphine-loaded HAPs was observed to contain different peaks  
 280 ( $653.32, 789.75, 875.36, 1653.8, 3473, 3539\text{ cm}^{-1}$ ) due to the morphine when compared to the  
 281 spectrum of HAP (Fig 2).



282

283

284 **Figure 2 FTIR spectrum of morphine loaded HA and unloaded HAPs, respectively.**

285

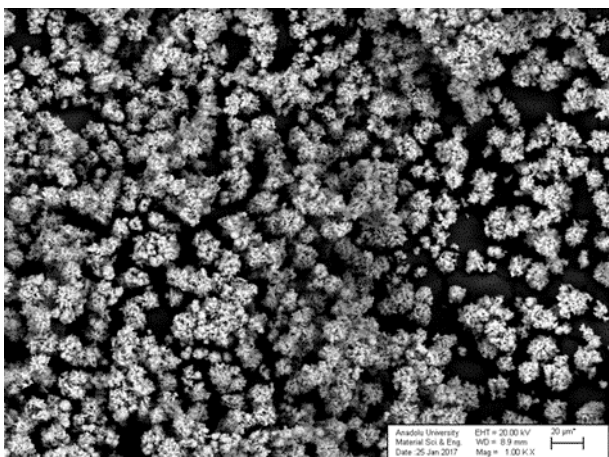
286 **3.3. Scanning electron microscopy**

287 Studies show that the morphology (Irregular, sphere, rod, needle, platelet, tube, fiber,  
 288 filament, wire, whisker, strip, platelet, flower) and magnitude of HAP (3 nm sp 1000 μm.)  
 289 may vary depending on the synthesis method used [26-28,].

290

291 The morphologies of the synthesized powders were observed by SEM and it was shown in  
 292 Fig. 3. The samples are mostly composed of fine-grained and homogeneous particles. The  
 293 produced spherical particles can be stacked at high levels, most of the particles are submicron  
 294 and nano-sized, as shown in Fig. 3. Since HA provides a porous surface structure, the  
 295 predominant size of the particles is in the range of 90-150 nm.

296



297

298 **Figure 3 SEM image of morphine loaded HAPs**

299

300 The crystal structures of apatite have been studied in details [29]. The HAP lattice consists of  
301  $\text{Ca}^{2+}$ ,  $\text{PO}_4^{3-}$  and  $\text{OH}^{1-}$  ions distributed over two mirror symmetric halves of the unit cell [30].

302 As a result of point analysis, Ca and P ions were detected in unloaded HAP as seen in figure

303 4. These ions in the structure of hydroxyapatite [ $\text{Ca}_5(\text{PO}_4)_3(\text{OH})$ ] are proof that the desired

304 HAP is formed as shown in figure 5. The structure of morphine ( $\text{C}_{17}\text{H}_{19}\text{NO}_3$ ) contains

305 nitrogen ions as seen in figure 5. As a result of the SEM point analysis, the determination of

306 the nitrogen with loaded particles has shown that morphine is loaded into HAP (fig 4). In this

307 study, SEM point analysis shows that both the empty HAP and the morphine loaded HAP

308 were obtained.

309

310 There are few articles describing the binding mechanisms of drug active substances on the  
311 surface of HAP particles. Therapeutic agents can interact with the surface of the nanoparticles

312 in two different ways. One is through detachable covalent connections and the other through

313 physical interactions. The amino or hydroxyl groups on the surface of the nanoparticles are

314 effective in covalent binding. Physical interactions such as electrostatic,

315 hydrophobic/hydrophilic and affinity ones can lead to coupling of drug molecules with the

316 surfaces of nanoparticles [31].

317

318 In a single cell unit of HAP, there are 10  $\text{PO}_4^{3-}$  groups of a unit cell, two remain inside and  
319 eight at the periphery. The positively charged morphine molecules we have obtained are most

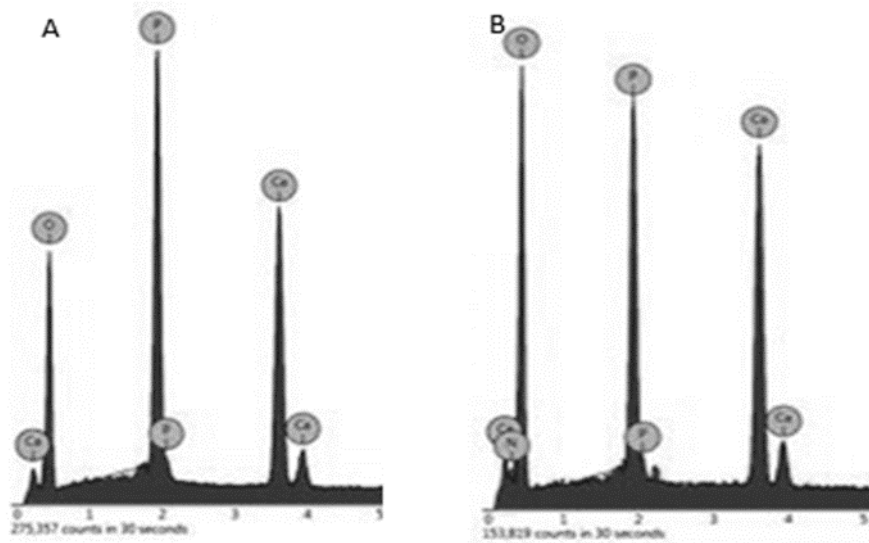
320 likely bound by weak electrostatic bonds within the hexagonal structure of the HAP

321 nanoparticles. Binding occurred between the negative charges of the polarized morphine ends

322 and the positively charged phosphate ions in the HAP.

323

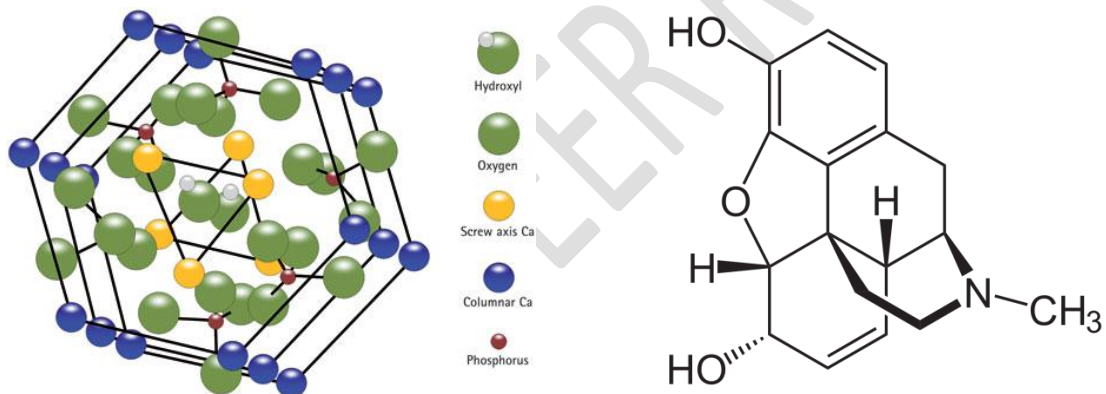
324



325

326 A; HAPs B; HAP+M

327 **Figure 4** Point analysis of empty (A) and morphine loaded (B) nanoparticle



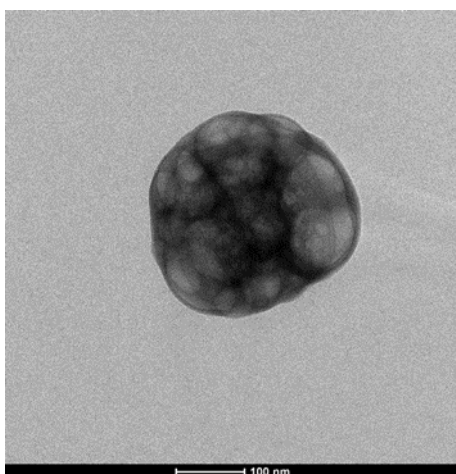
328

329 **Figure 5.** Chemical **structure** of HA and morphine

330

### 331 3.4. Transmission electron microscopy

332 Figure 6 shows TEM images of morphine loaded HA nanoparticle samples. The results  
333 demonstrated that the shape of morphine loaded HA nanoparticle samples is a spherical  
334 shape. Nanoparticle sizes were observed to be average 100 nm.



335

336 **Figure 6. TEM images of morphine loaded HA nanoparticle samples.**

337

### 338 **3.5. Comet Assay**

339 Since genotoxicity tests of many commonly used drugs are found to be positive, it has  
340 become mandatory to screen for mutagenic and carcinogenic potentials of new drugs. It has  
341 been reported that morphine causes a significant increase in micronucleus count and DNA  
342 damage depending on the dose [32]. Morphine **has** a genotoxic effect through reactive oxygen  
343 species (ROS) causing oxidative stress like other opioids [33-35]. In addition, **Morphine**  
344 causes DNA damage by inhibiting oxidative stress enzymes such as Glutathione peroxidase,  
345 Glutathione, Superoxide dismutase [36].

346

347 There is clear evidence that drugs can lead to oxidative stress. Oxidation on DNA results in  
348 various lesions such as abasic zones and single or double helix fractures.

349

350 There is clear evidence to implicate drug-induced oxidative stress as a mechanism of toxicity.  
351 Oxidation of DNA leads to the formation of lesions including oxidized bases, abasic sites, and  
352 DNA single- and/or double-strand breaks. One of the reliable techniques for determining  
353 oxidative DNA damage is single-cell gel electrophoresis (comet) assay [37]. COMET test is  
354 preferred by a number of researchers in toxicity studies due to its precision, speed and  
355 economy. In particular, showing DNA damage is a very useful and successful technique.  
356 *Shafer et al. (1994)* observed dose dependent, significant increases in the frequency of comet  
357 tails of fragmented DNA when cells were treated with morphine ( $5 \times 10^{-9}$  /  $10^{-7}$  M.) [38].

358 **Even though indirect measurements of oxidative stress level indicates the generation of ROS**  
359 **by HAP, no significant effects associated with ROS mediated cellular damage was evident**

360 suggesting the levels of ROS generated is not crossing the threshold level which the system  
361 could manage [39].

362  
363 In this study, the genotoxic effect of morphine-loaded HAP (HAP+M) was evaluated by  
364 measuring the values of both comet and oxidative stress parameters (TAS, TOS and OSI).  
365 The effect of HAP and HAP+M on DNA damage is given to Table 2. All tested  
366 concentrations increased DNA damage in a dose-dependent manner for HA ( $r=-0.891p=0.01$ )  
367 and for HAP+M ( $r=-0.905 p=0.01$ ). The significant DNA damage was induced after HA  
368 except for 5 mg/mL and after HAP+M at 25 mg/mL. While the highest DNA damage was  
369 observed the positive control ( $271.67\pm4.37$ ), the lowest one observed in the control group  
370 ( $0.33\pm0.33$ ). 25 mg/L of HAP+M significantly reduced DNA damage compared to HAP.

371

372 **Table 2 Protective effect of HO leaf extract against to H<sub>2</sub>O<sub>2</sub>**

373

374

Treatment	DNA Damage (Arbitrary Unit $\pm$ SD)*
Control	$0.33\pm0.33^a$
30 $\mu$ M H <sub>2</sub> O <sub>2</sub>	$271.67\pm4.37^b$
25 mg/L HAP	$110.67\pm2.33^c$
10 mg/L HAP	$8.33\pm0.67^d$
5 mg/L HAP	$1.67\pm0.33^{ae}$
25 mg/L HAP+M	$6\pm0.67^{de}$
10 mg/L HAP+M	$1\pm0.58^{ae}$
5 mg/L HAP+M	-

375 \* Means with the same letter do not differ statistically at the level of 0.05. SD: Standard Deviation

376 HAP; HA nanoparticle, HAP+M; morphine loaded HA nanoparticle

377

378 No significant difference was observed between the 5 mg / mL HAP + M and control group.  
379 When the concentration increased, total oxidant capacity increased and total antioxidant  
380 capacity decreased. 10 and 25 mg / mL of HAP and 25 mg / mL of HAP + M were found to  
381 be statistically significant compared to the control group (Table 3).

382

383 **Table 3. Total oxidant and antioxidant capacity**

	TAS (mmol Trolox Equiv./ L.)	TOS (mM H <sub>2</sub> O <sub>2</sub> Equiv. / L.)	OSI
Control	19.14±3.15 <sup>a</sup>	5.54±0.17 <sup>a</sup>	3.54±0.17 <sup>a</sup>
30 µM H <sub>2</sub> O <sub>2</sub>	5,21±0,25 <sup>b</sup>	19±4,25 <sup>b</sup>	10.54±0.15 <sup>b</sup>
25 mg/ mL HAP	8,12±0,21 <sup>c</sup>	14±1,23 <sup>c</sup>	8.21±0.49 <sup>c</sup>
10 mg/ mL HAP	12±1,71 <sup>d</sup>	10±1,51 <sup>d</sup>	5.95±0.18 <sup>d</sup>
5 mg/ mL HAP	16,57±0,41 <sup>a,c</sup>	7,01±1,11 <sup>a,c</sup>	4.52±0.6 <sup>a,c</sup>
25 mg/mL HAP+M	15,90±1,11 <sup>c,d</sup>	8,10±1,11 <sup>c,d</sup>	6.04±0.78 <sup>d</sup>
10 mg/mL HAP+M	18,11±1,47 <sup>a,c</sup>	5,11±0,47 <sup>a,c</sup>	5.4±2.11 <sup>c</sup>
5 mg/mL HAP+M	20,13±1,05 <sup>a</sup>	4,15±0,15 <sup>a</sup>	3.65±0.73 <sup>a</sup>

384

385

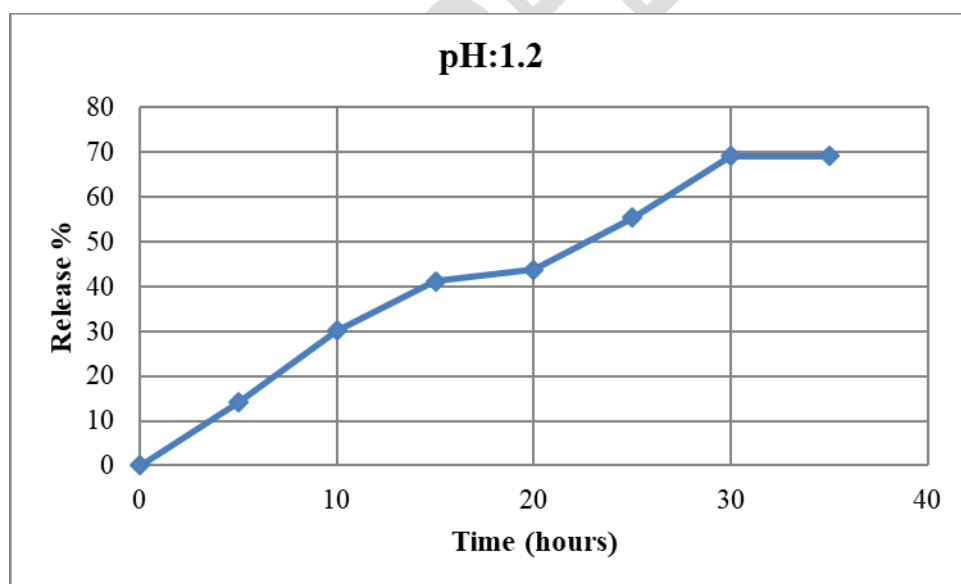
### 386 3.7. The effect of pH on morphine-loaded HAP release

387

388 The graph showing drug release in pH:1.2 as a function of time was given in Figure 7.

389 Morphine-loaded HAPs were found to release a maximum of 69.3 % at the end of 30 hours in  
390 pH:1.2.

391

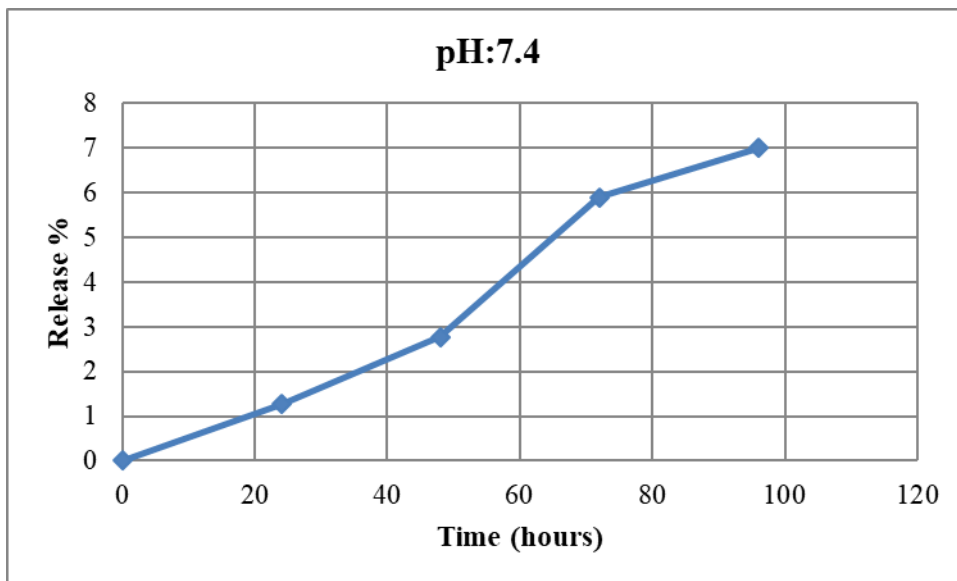


392

393 **Figure 7 The graph showing drug release in pH:1.2.**

394 The graph showing drug release in pH:7.4 as a function of time was given in Figure 8.

395 Morphine-loaded HAPs were found to release a maximum of 7.0 % at the end of 95 hours in  
396 the intestinal environment.



397

398

399 **Figure 8 The graph showing drug release in the intestinal environment.**

400

401 *Matsumoto et al (2004)* reported that release of protein in pH 4.0 was higher than pH 7.0 at  
 402 protein loaded HAP. This is because solubility of HA is greatly affected by the pH. In general,  
 403 a more acidic environment causes to become more soluble of HA, while a less acidic  
 404 environment makes HA less soluble.

405

#### 406 4. Conclusion

407

408 The development of morphine-based controlled release formulations for chronic pain  
 409 management is an extremely important issue. Other options should be used for drug delivery  
 410 aiming at obtaining effective, safe and innovative products. The literature has shown that  
 411 binding of morphine to particulate systems not only provides sustained and controlled release  
 412 of the drug but also provides a superior or equivalent analgesic profile and reduced side effect  
 413 formation from free radicals. HA appears to be an interesting alternative to future studies,  
 414 considering the wide range of advantages of nanoparticles and the lack of study of morphine.  
 415 Current studies are still not enough to revive the production of new products containing  
 416 morphine-loaded nanoparticles in the pharmaceutical industry.

417

418 In this study, it was determined that HAP can be used as a nongenotoxic morphine transport  
 419 system. However, the drug load of the carrier can be increased and controlled release is



420 achieved with modifications to the HAP molecule. Subsequent studies should be based on  
421 release modeling of the morphine charged HAP nanoparticle at in vivo and invitro media.

422

#### 423 **Disclaimer regarding Consent/Ethical Approval:**

424 As per university standard guideline participant consent and ethical approval has been  
425 collected and preserved by the authors.

426

#### 427 **REFERENCES**

428

- 429 1. Kroenke K, Krebs E, Wu J, Bair MJ, Damush T, Chumbler N, et al. Stepped care  
430 to optimize pain care effectiveness (scope) trial study design and sample  
431 characteristics. *Contemp Clin Trials*. 2014; 34: 270-281
- 432 2. Martin C, De Baerdemaeker A, Poelaert J, Madder A, Hoogenboom R, Ballet S.  
433 Controlled-release of opioids for improved pain management. *Materials Today*. 2016;  
434 19(9): 491–502
- 435 3. Woodle MC. Sterically stabilized liposome therapeutics. *Adv. Drug Deliv. Rev.* 1995;  
436 16(2–3): 249–265
- 437 4. Anselmo AC, Mitragotri S. (2014). Cell-mediated delivery of nanoparticles: Taking  
438 advantage of circulatory cells to target nanoparticles. *J. Control. Release*. 2014; 190:  
439 531–541.
- 440 5. Rossi F, Ferrari R, Papa S, Moscatelli D, Casalini T, Forloni G, Perale G, and  
441 Veglianese P. Tunable hydrogel-Nanoparticles release system for sustained  
442 combination therapies in the spinal cord. *Colloids Surfaces B Biointerfaces*. 2013;  
443 108:169–177
- 444 6. Choi YS, Lee MY, David AE, Park YS. Nanoparticles for gene delivery: therapeutic  
445 and toxic effects. 2014; *Mol. Cell. Toxicol.* 10 (1): 1–8
- 446 7. Bao G, Mitragotri S and Tong, S. Multifunctional nanoparticles for drug delivery and  
447 molecular imaging. *Annu. Rev. Biomed. Eng.* 2013; 15:253–82
- 448
- 449 8. Khaled RM, Hanan HB, Zenab M El-Rashidy. In vitro study of nano-  
450 HA/chitosan–gelatin composites for bio-applications. *Journal of Advanced*  
451 *Research* . 2014; 5: 201–208
- 452 9. Wang F, Li M, Lu Y. A simple sol-gel technique for preparing HA  
453 nanopowders. *Mater. Lett.* 2005; 59:916-919

- 454 10. Kim I, Kumta PN. Sol-gel synthesis and characterization of nanostructured HA  
455 powder. *Mater. Sci. Eng. B.*2004; 111: 232-236
- 456 11. Sun Y, Guo G, Wang Z, Guo H. Synthesis of single-crystal HAP nanorods. *Ceram.*  
457 *Int.* 2006; 32: 951-954
- 458 12. Koumoulidis GC, Katsoulidis AP, Ladavos AK, Pomonis PJ, Trapalis CC, Sdoukos  
459 AT, Vaimakis TC. Preparation of HA via microemulsion route. *J. Colloid Interface*  
460 *Sci.* 2003; 259: 254-260
- 461 13. Yin G, Liu Z, Zhan J, Ding F. and Yuan N. Impacts of the surface charge property  
462 on protein adsorption on HA. *Chemical Engineering Journal.* 2002; 87(2): 181– 186.
- 463 14. Kramer E, Podurgiel J and Wei M. Control of HA nanoparticle morphology using wet  
464 synthesis techniques: Reactant addition rate effects. *Materials Letters.*2014; 131: 145 –  
465 147.
- 466 15. Mostafa AA, Oudadesse H, Mohamed MB, Foad ES, Le Gal Y and Cathelineau G.  
467 The convenient approach of nanoHA polymeric matrix composites. *Chemical*  
468 *Engineering Journal.* 2009; 153(1): 187 – 192.
- 469 16. Taş CA, Korkusuz F, Timuçin M, Akkaş N. An investigation of the chemical  
470 synthesis and high-temperature sintering behaviour of calcium HA and tricalcium  
471 phosphate (TCP) bioceramics. *J Mater Sci Mater Med.*1997; 8:91-6.
- 472 17. Endlová L, Laryšová A, Vrbovský V, Navrátilová Z. Analysis of Alkaloids in Poppy  
473 Straw by High-Performance Liquid Chromatography, *IOSR Journal of Engineering.*  
474 2015; 05:1-7.
- 475 18. Gün M. Aljinat-Kitosan Nanopartiküllerin Kolşisin Salımında Kullanılmasının  
476 Araştırılması, Yüksek Lisans, Kimya Anabilim Dalı Programı Adnan Menderes  
477 Üniversitesi Fen Bilimleri Enstitüsü.2013
- 478 19. Singh NP, McCoy MT, Tice RR, Schneider EL. A simple technique for quantitation  
479 of low levels of DNA damage in individual cells. *Exp Cell Res.* 1988; 175:184– 191.
- 480 20. Avuloğlu Y, Yüzbaşıoğlu D. Evaluation of genotoxic effects of 3-methyl-5-(4-  
481 carboxycyclohexylmethyl)-tetrahydro-2H-1,3,5-thiadiazine-2-thione on human  
482 peripheral lymphocytes. *Pharmaceutical biology,*2017; 55(1): 1228–1233
- 483 21. Ciğerci IH, Liman R, Özgül E, Konuk M. Genotoxicity of indiumtin oxide by Allium  
484 and Comet tests. *Cytotechnology.* 2015; 67:157–163
- 485 22. Feng W, Li MS, Lu YP. and Qi YX, Liu YX. Synthesis and microstructure of HA  
486 nanofibers synthesized at 37oC, *Materials Chemistry and Physics.*2006; 95: 145-149

- 487 23. Cengiz B. Hidroksiapatit Nanoparçacıklarının Sentezi, Yüksek Lisans, Kimya  
488 Mühendisliği Anabilim Dalı, Fen Bilimleri Enstitüsü. 2007
- 489 24. Misra N, Dwivedi , Pandey AK and Trived S. Vibrational analysis of Two Narcotic  
490 Compounds- Codeine and Morphine - A comparative DFT study. *Der Pharma.*  
491 *Chemica.*2011; 3(3):427-448
- 492 25. Padmanabhan SK, Balakrishnan A, Chu MC, Lee YJ, Kim TN, Cho SJ. Sol-gel  
493 synthesis and characterization of HA nanorods. *Particuology.* 2009;7:466-470.
- 494 26. Shojai MS, Khorasani MT, Khoshdargi ED, Jamshidi A. Synthesis methods for  
495 nanosized HA with diverse structures. *Acta Biomater.* 2013; 9:7591-7621
- 496 27. Mobasherpour I, Heshajin MS, Kazemzadeh A, Zakeri M. Synthesis of  
497 nanocrystalline HA by using precipitation method. *J Alloys Compd.* 2007; 430:330-  
498 333.
- 499 28. Naray SS. The structure of apatite  $(\text{CaF})\text{Ca}_4(\text{PO}_4)_3$ . *Z Kristallogr.* 1930; 75:387-398.
- 500 29. Mondal S, Dorozhkin S, Pal U. Recent progress on fabrication and drug delivery  
501 applications of nanostructured HA .*Wiley Interdiscip Rev Nanomed*  
502 *Nanobiotechnol.*2018;10(4): doi: 10.1002/wnan.1504.
- 503 30. Kong L, Mu Z, Yu Y, Zhang L, Hu J. Polyethyleneimine- stabilized HAPs modified  
504 with hyaluronic acid for targeted drug delivery. *RSC Adv* 2016, 6:101790-101799.
- 505 31. Li Jih-Heng and Lin Lih-Fang .Genetic toxicology of abused drugs: a brief review.  
506 *Mutagenesb* vol.13 no.6 pp.557-565, 1998
- 507 32. Zhang YT, Zheng QS, Pan J, Zheng RL. Oxidative damage of biomolecules in mouse  
508 liver induced by morphine and protected by antioxidants. *Basic Clin Pharmacol*  
509 *Toxicol.* 2004; 95:53-8.
- 510 33. Sharp BM, Keane WF, Suh HJ, Gekker G, Tsukayama D, Peterson PK. Opioid  
511 peptides rapidly stimulate superoxide production by human polymorphonuclear  
512 leukocytes and macrophages, *Endocrinology.* 1985; 117:793-5.
- 513 34. Slupphaug G, Kavli B, Krokan HE. The interacting pathways for prevention and repair  
514 of oxidative DNA damage, *Mutat Res.* 2003; 531:231-51.
- 515 35. Skoulis NP, James RC, Harbison RD, Roberts SM. Depression of hepatic glutathione  
516 by opioid analgesic drugs in mice. *Toxicol Appl Pharmacol.* 1989; 99:139-47.
- 517 36. Damian GD, Elizabeth AM, Judith MH, and Ruth R. Drug-Induced Oxidative Stress  
518 and Toxicity. *J Toxicol.* 2012, Article ID 645460, 13 pages. doi:  
519 10.1155/2012/645460

- 520 37. Shafer DA , Xie Y. Detection of opiate- enhanced increases in DNA damage, HPRT  
521 mutants, and the mutation frequency in human HUT- 78 cells. Environmental and  
522 Molecular Mutagenesis. 1994; 23:37-44.
- 523 38. Remya NS, Syama S, Sabareeswaran A, Mohanan PV. Investigation of chronic  
524 toxicity of hydroxyapatite nanoparticles administered orally for one year in wistar rats.  
525 Materials Science and Engineering: C.2017; 76: 518-527

526

527

528

529

530

UNDER PEER REVIEW